



ELSEVIER

Journal of Chromatography A, 890 (2000) 25–36

JOURNAL OF  
CHROMATOGRAPHY A

www.elsevier.com/locate/chroma

# High-performance chromatofocusing using linear and concave pH gradients formed with simple buffer mixtures

## I. Effect of buffer composition on the gradient shape<sup>☆</sup>

Ronald C. Bates<sup>1</sup>, Xuezhen Kang, Douglas D. Frey\*

*Department of Chemical and Biochemical Engineering, University of Maryland Baltimore County, Baltimore, MD 21250, USA*

### Abstract

Numerical calculations together with simplified analytical relations based on local equilibrium theory are used to determine the factors which govern the shape of the gradient formed during chromatofocusing when simple mixtures of buffering species are employed to produce linear or concave pH gradients. The numerical and analytical development is also used to determine the relation between the gradient shape and the buffering capacities of the adsorbed and liquid phases. Experiments which verify the theoretical methods are described where internally generated, retained pH gradients of various shapes are formed using high-performance chromatography columns. The resulting experimental and theoretical basis can be employed as means for the selection of the buffer composition for use in chromatofocusing. © 2000 Elsevier Science B.V. All rights reserved.

*Keywords:* Chromatofocusing; pH gradients; Buffer composition; Gradient elution

### 1. Introduction

Chromatofocusing was originally developed by Sluyterman and co-workers [1–4] and is most commonly applied to the separation of proteins. To perform the method, an internally generated pH gradient is made to propagate inside an ion-exchange chromatography column as a retained front due to the adsorption behavior of the buffering species in the elution buffer. The method as typically practiced employs a weak-base, anion-exchange column packing and a polyampholyte elution buffer containing a

mixture of polymeric buffering species that buffers a broad pH range.

Although the technique of chromatofocusing as just described has yielded considerable success in separating proteins, the use of polyampholyte buffers is perhaps the greatest limitation of the method. In particular, these types of buffers add considerably to the expense of using chromatofocusing and have chemical compositions that tend to vary from batch to batch as obtained from chemical suppliers. Shallow pH gradients formed with polyampholyte buffers also tend to be irregular and irreproducible in shape and may yield poor separations [5]. In addition, in preparative applications the removal of polyampholytes from the purified product is often difficult since they tend to form association complexes with proteins [6].

Due to the limitations of using polyampholyte elution buffers, various workers have investigated

<sup>☆</sup>Part II: X. Kang, R.C. Bates, D.D. Frey, J. Chromatogr. A, 890 (2000) 37.

\*Corresponding author. Tel.: +1-410-4553-400; fax: +1-410-4551-049.

E-mail address: dfrey1@umbc2.umbc.edu (D.D. Frey).

<sup>1</sup>Present address: Pfizer Inc., Groton, CT, USA.

methods for replacing these buffers with a chemically well defined mixture of low-molecular-mass buffering species. For example, Hearn and Lyttle [7] and Hutchens et al. [8,9] have investigated the use of a large number of low-molecular-mass buffering species in the elution buffer. Under these conditions, the effluent pH profile consists of a sequence of discrete pH steps spanning the elution pH and presaturation (i.e., starting) pH, with the number of steps corresponding to the number of adsorbed buffering species in the elution buffer. Nevertheless, if an adequate number of these buffering species is present, the pH profile becomes sufficiently close to linear in shape so that the method operates essentially the same as when a polyampholyte elution buffer is employed. Liu and Anderson [10,11] have described related work in which gradual, retained pH gradients are produced with a limited number of buffering species in the elution buffer by using external mixing of two different elution buffers to aid in the formation of the gradient.

Another approach to simplify the elution buffer suitable for preparative-scale chromatofocusing has been described by Frey [12] and Strong and Frey [13] in which either a weak- or strong-base ion-exchange column packing is used together with a minimal number of low-molecular-mass buffering species in the elution buffer. These workers demonstrated that when buffering species are optimally chosen, the protein of interest can be selectively focused on a single, retained self-sharpening pH front in the column effluent while the impurities elute from the column in other regions of the pH profile.

A final method to eliminate the use of polyampholyte buffers is based on the original observation of Sluyterman and Wijdenes [3,4] that a retained, gradual pH gradient can be produced using a weak-base anion-exchange column packing if the presaturation and elution buffers contain only neutral or positively charged species, i.e., if amine buffering species are employed, so that none of the buffering species adsorb to any great extent onto the column packing. Sluyterman, however, did not pursue the development of this method, but instead opted to investigate systems where external mixing was used to augment the formation of the pH gradient or where polyampholyte buffers were used. Recently,

this method was re-examined by Bates and Frey [14] and Logan et al. [15] who both investigated methods for obtaining pH gradients of an appropriate shape using simple mixtures of buffering species in the elution buffer and without the use of external mixing. However, this work involved only low-pressure chromatography and the suitability of the method when high-performance column packings and instrumentation are employed was not investigated. Related work which has apparently never been published has also been described by Kirsh [16].

The goal of the present work is to extend the method of Bates and Frey [14] and demonstrate that useful protein separations can be accomplished using high-performance column packings with the strategy described in that study. In Part I of this work, the application of high-performance chromatofocusing using simple mixtures of buffering species in the elution buffer will be evaluated with regard to the shape of the pH profile attained, and a means will be developed for the rational design of these buffer mixtures. In Part II, the method will be further evaluated with regard to the resolution and speed achieved when separating protein mixtures. The results of the present work apply not only to analytical chromatography, but also to preparative chromatography where the focusing effect inherent in chromatofocusing and the high mass transfer efficiency that results from using high-performance column packings can be exploited together to isolate and purify proteins.

## 2. Experimental

The species used to make buffer solutions (diethanolamine, imidazole, Tris, Bis-Tris, piperazine and *N*-methylpiperazine) were obtained from Sigma (St. Louis, MO, USA). The buffer solutions were filtered and degassed by vacuum filtering using a 0.2- $\mu\text{m}$  pore size, 47 mm diameter filter composed of nylon 66 (Rainin, Ridgefield, NJ, USA). The buffers were made by adding a known mass of each buffering species to a known volume of filtered, deionized water. This volume was typically 90% of the desired final volume. The solution was then titrated with hydrochloric acid to the appropriate pH. After the desired pH was attained, an additional volume of

filtered deionized water was added to yield the desired final solution volume. The final solution was then vacuum filtered through a 0.2- $\mu\text{m}$  membrane filter.

Low-pressure chromatofocusing was performed using PBE 94 stationary phase (Amersham Pharmacia Biotech, Piscataway, NJ, USA) which was packed into a 10 $\times$ 1 cm I.D. glass column (Omnifit, Cambridge, UK). High-performance chromatofocusing was performed using a 5 $\times$ 0.5 cm I.D. Mono P column, also obtained from Amersham Pharmacia Biotech. The chromatography equipment used was either a Model P4000 SpectraSystem pump and a Model UV2000 SpectraSystem UV–Vis absorbance detector (Thermo Separation Products, San Jose, CA, USA), or a Model 510 HPLC pump and a Model 490E programmable absorbance detector (Waters, Milford, MA, USA). The pH of the eluent was measured using a low-volume on-line sampling cell and a Model 450 pH electrode (Sensorex, Stanton, CA, USA) attached to a Model 701A Ionanalyzer (Orion, Beverly, MA, USA). To perform an experiment, the column was first equilibrated with the presaturation buffer until the presaturation pH was measured at the column outlet. The mobile phase flowing through the column was then switched to the elution buffer to begin the formation of the gradient.

### 3. Effect of elution buffer composition on the pH gradient shape

#### 3.1. General relations

Consider the case where a column containing an ion-exchange column packing is uniformly presaturated at a given pH, where elution is carried out by a stepwise change to an elution buffer, and where a single ionic species is present which has the proper charge type to adsorb onto the column packing. Assume also that the adsorbing ionic species is inert in the sense that it is either the conjugate base of a strong acid, or the conjugate acid of a strong base, so that it does not participate in acid–base equilibrium. As discussed by Bates and Frey [14], if local equilibrium is assumed to exist between the liquid and adsorbed phases throughout the column, then a differential material balance for the inert ionic

species inside the column yields the following relation for the time at which a pH value exits the column:

$$t(\text{pH}) = (L/v_{\text{fluid}}) \cdot \left[ 1 + \frac{(1-\alpha)}{\alpha} \cdot \frac{dq_{S,t}^*}{dC_S} \right] \quad (1)$$

In Eq. (1), the superscript ‘\*’ denotes an equilibrium value so that the term  $dq_{S,t}^*/dC_S$  is the slope of the adsorption isotherm for the inert ion  $S$  at the given pH in a liquid phase containing the buffering species at their concentrations in the elution buffer. Note that the subscript  $t$  in Eq. (1) indicates that the adsorbed phase concentration is determined as the amount of ion  $S$  within the exterior surface of the particle per unit volume and that the term inside the square brackets in Eq. (1) is large compared to unity for the situation of most interest where the gradient is strongly retained by the column packing, in which case  $t(\text{pH})$  is directly proportional to  $dq_{S,t}^*/dC_S$ . Note also that Eq. (1) applies to the case where the gradient is gradual in nature, i.e., nonself-sharpening. If an abrupt (i.e., self-sharpening) pH transition occurs, a discontinuous version of Eq. (1) must be employed, as discussed by Bates and Frey [14].

The term  $dq_{S,t}^*/dC_S$  in Eq. (1) can be written in the following form:

$$\frac{dq_{S,t}^*}{dC_S} = \frac{dq_{S,t}^*/dpH_{\text{fluid}}}{dC_S/dpH_{\text{fluid}}} \equiv \frac{\beta'_{\text{ads}}}{\beta_{\text{fluid}}} \quad (2)$$

where  $dC_S/dpH_{\text{fluid}}$  is the buffering capacity in the liquid phase, i.e.,  $\beta_{\text{fluid}}$ . The term  $dq_{S,t}^*/dpH_{\text{fluid}}$  in Eq. (2), which is also denoted as  $\beta'_{\text{ads}}$ , is the change in the inert ion concentration in the adsorbed phase per unit change in the liquid phase pH in the presence of the elution buffer. The relation between  $\beta'_{\text{ads}}$  and  $\beta_{\text{ads}}$ , the latter being the buffering capacity of the adsorbed phase (i.e.,  $dq_{S,t}^*/dpH_{\text{ads}}$ , where  $pH_{\text{ads}}$  is the pH in the adsorbed phase), and the relation between  $\beta'_{\text{ads}}$  and the usual convention for measuring the titration curve of the column packing (i.e.,  $\beta''_{\text{ads}}$ , defined as the change in the inert ion concentration in the adsorbed phase per unit change in the liquid phase pH in the presence of a constant and excess concentration of the inert ion in the liquid phase), is discussed below.

Bates and Frey [14] used Eqs. (1) and (2) by calculating  $\beta_{\text{fluid}}$  using dissociation constants for the

buffering species taken from the literature and by using a model for the adsorbed phase to infer  $\beta'_{\text{ads}}$  from measurements of  $\beta''_{\text{ads}}$ . Although Bates and Frey were able to use Eqs. (1) and (2) in this manner to interpret various features of experimentally measured pH gradients, such as the formation of composite pH fronts having both self-sharpening and nonself-sharpening sections, it is often difficult to determine the buffering capacities needed in Eqs. (1) and (2) precisely enough to yield accurate predictions of the pH gradient shape. For this reason, in this study Eqs. (1) and (2) will be used quantitatively only to interpret numerical studies of the effect of the elution buffer compositions on the shape of pH gradient. However, to interpret experimental data  $\beta_{\text{fluid}}$  will be determined from literature values of the dissociation constants for the buffering species in the elution buffer,  $\beta'_{\text{ads}}$  will be inferred from the shape of the pH profile, and Eqs. (1) and (2) will then be used on a more qualitative basis. For this purpose it is useful to note that the buffering capacities of mono- and dibasic buffering species are given, respectively as follows [17]:

$$\beta_{\text{fluid, monobasic}} = 2.303 \cdot \frac{C_{\text{buffer}} K_{\text{a}} C_{\text{H}^+}}{(K_{\text{a}} + C_{\text{H}^+})^2} \quad (3)$$

$$\beta_{\text{fluid, dibasic}} = 2.303 \cdot C_{\text{buffer}} K_{\text{a1}} C_{\text{H}^+} \cdot \frac{C_{\text{H}^+}^2 + 4K_{\text{a2}} C_{\text{H}^+} + K_{\text{a1}} K_{\text{a2}}}{(C_{\text{H}^+}^2 + K_{\text{a1}} C_{\text{H}^+} + K_{\text{a1}} K_{\text{a2}})^2} \quad (4)$$

In Eq. (3),  $C_{\text{buffer}}$  is the concentration of the buffering species counting all its charged forms and  $K_{\text{a}}$  is the dissociation constant for the following equilibrium relation for a monobasic species:



Similarly,  $K_{\text{a1}}$  and  $K_{\text{a2}}$  in Eq. (4) are the dissociation constants for the following two equilibrium relations for a dibasic species:



### 3.2. Adsorption equilibrium for an inert ion

Consider an ionic species having a charge opposite

to that of the fixed charged groups on the column packing where the ionic species is inert in the sense described previously. Since at equilibrium the chemical potential of electrically neutral ion combinations is equal in the adsorbed and fluid phases, and since this chemical potential can be written as the product of the activities of the individual ions, the following expression applies [12,14,18]:

$$q_{\text{H}^+,t} q_{\text{S},t} = K_{\text{S},t} C_{\text{H}^+} C_{\text{S}} \quad (8)$$

In Eq. (8) the adsorption equilibrium parameter  $K_{\text{S},t}$  includes the activity coefficients of the hydrogen and inert ions in the liquid and adsorbed phases. The degree to which the functional groups attached to the column packing are ionized can be determined using the following expression which incorporates the acid–base equilibrium relations for the functional groups:

$$q_{\text{R}^+,t} = \sum_j q_{\text{R}^+,t} = \sum_j \frac{q_{\text{H}^+,t} q_{\text{R}_j,t}}{K_{\text{R}_j} + q_{\text{H}^+,t}} \quad (9)$$

If it is assumed that the hydrogen and hydroxide ion concentrations are small compared to the concentrations of other ions in the adsorbed phase, then the hydrogen ion concentration in the adsorbed phase can be determined by solving the following electro-neutrality condition which incorporates Eq. (8):

$$\frac{K_{\text{S},t} C_{\text{S}} C_{\text{H}^+}}{q_{\text{H}^+,t}} - \sum_j \frac{q_{\text{H}^+,t} q_{\text{R}_j,t}}{K_{\text{R}_j} + q_{\text{H}^+,t}} = 0 \quad (10)$$

Provided that the liquid phase composition is specified, then Eq. (10) can be solved for the hydrogen ion concentration in the adsorbed phase, which can then be substituted into Eq. (8) to determine the concentration of the inert ion in the adsorbed phase.

### 3.3. Numerical studies of the effect of buffer composition on the pH gradient shape

Figs. 1 and 2 illustrate results using the numerical methods described by Frey et al. [18] that show the effect of the elution buffer composition on the shape of the pH gradient. The numerical simulations shown account for the adsorption equilibrium of the inert ion using the relations described in Section 3.2 while

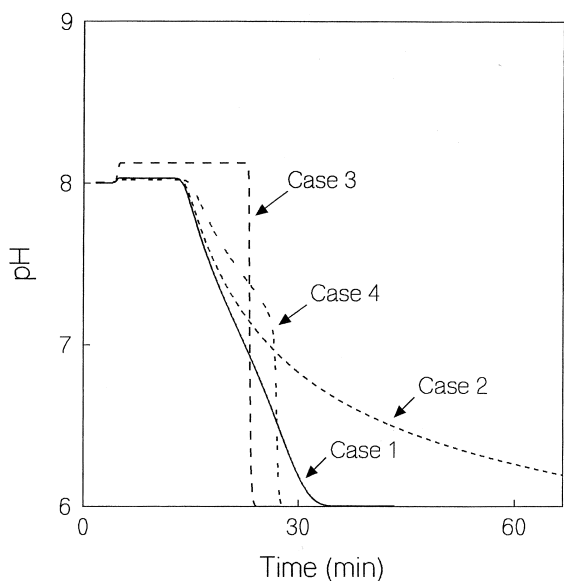


Fig. 1. Numerical calculations of the pH profile shape for various elution buffer compositions as described in Table 1. The column packing used in the calculations was assumed to incorporate three weak acid functional groups having  $pK_a$  values of 7.6, 8.6, and 9.6 with concentrations of 0.333 M each. In all of the cases the column was presaturated at pH 8 with the buffering species having a  $pK_a$  value of 8.0. The calculations assume a column length of 10 cm, a particle diameter of 35  $\mu\text{m}$ , a diffusion coefficient for the inert anion of  $10^{-6}$   $\text{cm}^2/\text{s}$ , an interstitial flow velocity of 0.1  $\text{cm}/\text{s}$ , an adsorption equilibrium constant for the inert anion of unity, and an interstitial porosity (or void volume) of 0.35.

the mass transfer behavior of the inert ion is accounted for using a linear driving force approximation as discussed by Frey et al. The conditions used for each of the cases shown in the figure are described in the figure caption and in Table 1. Note that in each of the cases the buffering species employed are weak bases that form neutral and positive ions, but not ions of the proper charge type to adsorb on the anion-exchange column packing used. The calculations shown also correspond to the case where the buffering capacity of the adsorbed phase is provided by three types of functional groups with dissociation constants as described in the figure caption.

Despite the idealized conditions used for the numerical simulations, Figs. 1 and 2 can nevertheless be used as a qualitative guide for the selection of the buffering species in the elution buffer to produce a

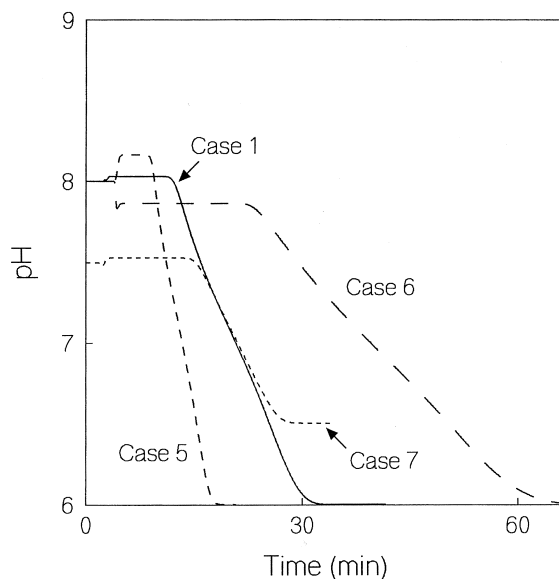


Fig. 2. Numerical calculations of the pH profile shape for various elution buffer compositions as described in Table 1. Conditions used are the same as in Fig. 1 except that for case 7 the presaturation and elution buffers were at pH 7.5 and 6.5, respectively.

pH gradient of a desired shape. For this purpose it is useful to first examine Fig. 3 which illustrates buffering capacities for the adsorbed and liquid phases as functions of the liquid phase pH for case 1. The buffering capacities for the liquid phase in Fig. 3 were determined using Eqs. (3) and (4) while the buffering capacities of the adsorbed phase were determined by numerical differentiation of the equilibrium expressions described in Section 3.2. As shown in the figure,  $\beta_{\text{ads}}$  and  $\beta'_{\text{ads}}$  are nearly equal to each other due to the fact that, in the determination

Table 1  
Molar concentrations of weak base buffering species used in the numerical simulations shown in Figs. 1 and 2

Case No.	Species 1 ( $pK_a=8$ )	Species 2 ( $pK_a=7$ )	Species 3 ( $pK_a=6$ )
1	0.1	0.0362	0.0362
2	0.1	0.0362	0
3	0	0.0724	0.0724
4	0.1	0	0.0724
5	0.2	0.0724	0.0724
6	0.05	0.0181	0.0181
7	0.1	0.0362	0.0362

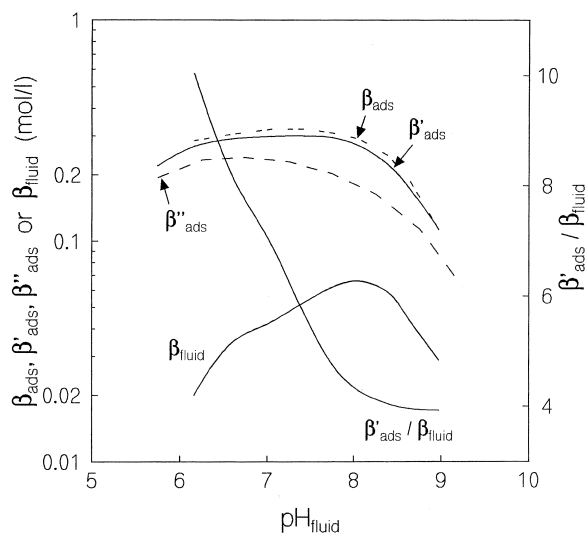


Fig. 3. Calculated values for the buffering capacities  $\beta_{\text{fluid}}$ ,  $\beta_{\text{ads}}$ ,  $\beta'_{\text{ads}}$ , and  $\beta''_{\text{ads}}$  as functions of the liquid phase pH for the conditions that correspond to case 1 in Fig. 1. The determination of  $\beta''_{\text{ads}}$  assumes that the liquid phase concentration of the inert ion is 0.2 M.

of  $\beta'_{\text{ads}}$ , the increase in the liquid phase ionic strength with pH caused by the titration of the buffering species in the liquid phase is nearly equal to the increase in the adsorbed phase ionic strength caused by the titration of the functional groups on the column packing. This implies that the ratio  $\text{d}pH_{\text{fluid}}/\text{d}pH_{\text{ads}}$  is near unity under these conditions. In contrast,  $\beta''_{\text{ads}}$  is seen to be significantly less than either  $\beta_{\text{ads}}$  or  $\beta'_{\text{ads}}$  due to the fact that in the determination of  $\beta''_{\text{ads}}$  it is assumed that the liquid phase ionic strength is fixed as the pH changes.

Fig. 3 also illustrates the variation in the ratio  $\beta'_{\text{ads}}/\beta_{\text{fluid}}$  with liquid phase pH for case 1. As shown, this ratio is seen to increase significantly as the pH decreases due mainly to a corresponding decrease in  $\beta_{\text{fluid}}$ . According to Eqs. (1) and (2), the nearly linear increase in  $\beta'_{\text{ads}}/\beta_{\text{fluid}}$  shown in Fig. 3 as the pH decreases should result in a nearly linear increase in the time for pH values to exit the column as the pH decreases, in agreement with the numerical calculations shown in Fig. 1. Fig. 3 also indicates that when the adsorbed phase has an even buffering capacity in the pH range of interest, it is necessary for the buffering capacity in the liquid phase to decrease as the pH decreases so that the ratio  $\beta'_{\text{ads}}/\beta_{\text{fluid}}$

$\beta_{\text{fluid}}$  increases in this direction. This is in contrast to the case where the buffering species are adsorbed, as for example when polyampholyte buffers are used, in which case an even buffering capacity for both the adsorbed and liquid phases is generally needed to attain a linear pH gradient [5].

The liquid phase buffering capacities as functions of pH for cases 1–4 are shown in Fig. 4 and can be used, together with Eqs. (1) and (2), to rationalize the effect of changes in buffer composition on the shape of the pH gradient. More specifically, as described above, Eqs. (1) and (2) indicate that if a certain selection of buffering species in the elution buffer yields a linear pH gradient, then the quantity  $\beta'_{\text{ads}}/\beta_{\text{fluid}}$  must be linearly related to the liquid phase pH. Under these conditions it follows that a change in the concentrations of the buffering species that causes the corresponding relative change in the liquid phase buffering capacity to also be a linear function of pH will yield a different but still linear pH gradient due to the fact that  $\beta'_{\text{ads}}/\beta_{\text{fluid}}$  will still be linearly related to pH for the new buffer composition. However, if the relative change in the liquid phase buffering capacity is proportionately greater or smaller in some region of the pH gradient as compared to a linear variation, a nonlinear pH

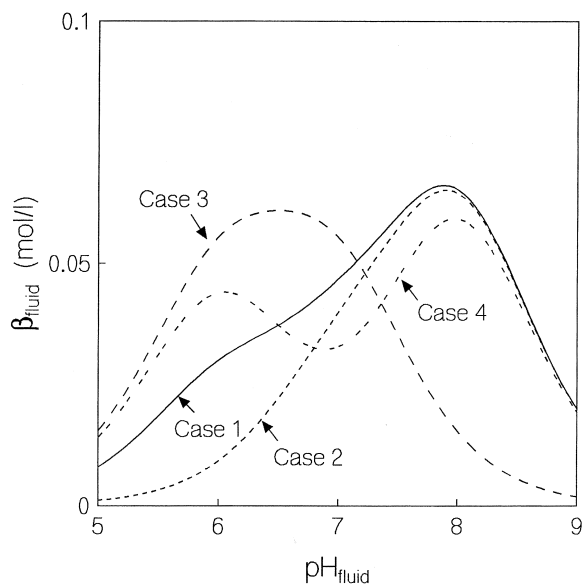


Fig. 4. Calculated buffering capacities of the liquid phases used for cases 1–4 in Fig. 1.

gradient will occur. For example, in comparison to case 1 in Fig. 4, there is a proportionately greater decrease in the liquid phase buffering capacity in the low-pH region as compared to the high-pH region in case 2 so that a concave pH gradient occurs in the latter case, as illustrated by the numerical calculations in Fig. 1. In contrast, case 4 in Fig. 4 illustrates the opposite situation where the decrease in liquid phase buffering capacity in the high-pH region is proportionately less than the decrease in the low-pH region (more specifically, the buffering capacity increases in this latter region) so that a composite pH front is formed which includes a stepwise transition in the low-pH region (case 4). Finally, case 3 is an extreme version of case 4 where the entire pH transition becomes stepwise in nature.

The effect of changes in the buffering capacity of the elution buffer caused by increasing the concentrations of all the buffering species by a fixed ratio, i.e., a uniform relative change in the buffering capacity across the entire pH gradient, is illustrated by the numerical calculations shown in Fig. 2. As shown, and as indicated by Eqs. (1) and (2), the result is a corresponding change in the steepness of the gradient, but not in its general shape. Fig. 2 also illustrates the effect of changing the pH of the elution and presaturation buffers, but with fixed concentrations for the buffering species in the elution buffer. The results indicate that reducing the pH range spanned by the gradient in this manner does not effect the times at which pH values exit the column, but instead a truncated gradient is formed in which the elution and presaturation pH plateaus are correspondingly increased.

#### 4. Selection of buffering species

Of the various types of gradients shown in Fig. 1, the two most useful for separating proteins are the linear (case 1) and the concave (case 2) gradients. Linear pH gradients are the type most commonly advocated for chromatofocusing since they often tend to minimize the separation time while also leading to high resolutions between elutes [19]. However, when a higher resolution is desired between later eluting bands, or when a pH gradient of a desired slope in a particular region of the pH profile

can be achieved even when the slope of the pH profile varies, then a concave pH profile or other nonlinear shape for the profile may lead to acceptable resolution [5].

Table 2 gives the  $pK_a$  values of several amine buffering species that can in principle be used to produce gradual pH gradients on an anion-exchange column packing using the strategy described above. The buffering species shown in the table are commonly used in chromatographic studies since they are readily available, tend not to interact with solid surfaces or proteins by hydrophobic binding, and do not absorb light at wavelengths where absorbance detection of proteins generally takes place. According to the reasoning pertaining to Fig. 1, these buffering species can be used to produce linear gradients that span the region between pH 9 and 5, and concave gradients that span the region between pH 9 and pH values below 5.

Although amine buffering species with  $pK_a$  values below 5 exist, these types of buffering species are much less commonly used in chromatographic studies, and tend to be large organic molecules that are likely to have physical properties which make it difficult to achieve a pH gradient of a desired shape. For example, buffering species of this type have a tendency to adsorb onto ion-exchange column packings due to hydrophobic binding and to have  $pK_a$  values that depend on temperature to a significant extent [20]. The lack of appropriate amine buffering species for use in chromatography with  $pK_a$  values below 5 generally leads to the selection of acidic buffering species in this region, as discussed by Liu and Anderson [10,11]. However, the use of acidic buffering species together with an anion-exchange column packing leads to the formation of stepwise, self-sharpening pH fronts, as opposed to the gradual pH fronts desired in this study [12]. For these

Table 2  
Properties of the amine buffering species used in this study

Buffering species	$pK_a$
Diethanolamine (DEA)	8.9
Tris	8.06
Imidazole	6.95
Bis-Tris	6.5
Piperazine	5.76, 9.72
<i>N</i> -Methylpiperazine	4.94, 9.09

reasons, in this study only the buffering species shown in Table 2 will be employed since past work indicates they behave in a predictable manner with regard to the formation of retained pH gradients [14]. Correspondingly, in this work linear or nearly linear pH gradients will be utilized in the pH region between pH 9.5 and 5 whereas concave pH gradients will be employed when the pH of the elution buffer is less than 5.

## 5. Column packing considerations

One factor that may need to be considered when producing a pH gradient with a simple buffer mixture is that for some column packings an irregularity in the pH profile may occur over certain pH ranges. Such behavior is not predicted by Eqs. (1) and (2), but instead is apparently due to as yet unexplained phenomena. Fig. 5 illustrates this type of behavior for PBE 94, which is a low-pressure column packing made specifically for chromatofocusing. As shown, when the column was presatu-

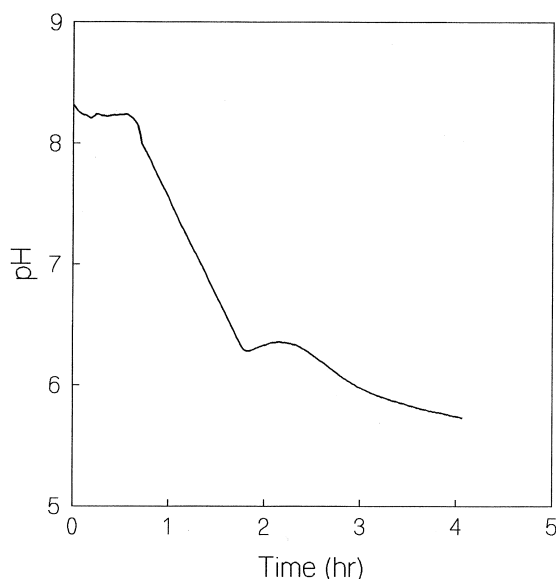


Fig. 5. Effluent pH profile obtained using a  $15 \times 1.0$  cm I.D. PBE column. The adsorbent was initially presaturated with 35 mM Tris at a pH of 8.2 and eluted with a buffer containing 35 mM Tris, 5 mM Bis-Tris, and 5 mM imidazole at pH 5.7 and at a flow-rate of 1.0 ml/min. Both the presaturation and elution buffers contained chloride as the only anion present.

rated at pH 8.2 and eluted at pH 5.8, a pH hump occurred at pH 6.2 in a gradient that is otherwise concave in shape. Similar behavior is illustrated in Fig. 6 for a Mono P high-performance column. As shown, when the presaturation pH is 8.2, a nearly linear pH gradient is produced when the elution pH is 6.5 or 6.0, but a plateau at pH 6.0 followed by a pH transition to the elution pH is produced when the pH of the elution buffer is further lowered to a value of 5.5.

Perturbations in the pH gradient as shown in Figs. 5 and 6 were first observed by Sluyterman and Wijdenes [3] when using a DEAE-Sepharose column packing. These workers postulated that this behavior resulted from a shift in the acid–base equilibrium behavior of the functional groups attached to the base material of the column packing, due in turn to a slow structural rearrangement of the base material as the functional groups changed their charge state. The fact that the PBE 94 low-pressure column packing used in Fig. 5 exhibits a larger gradient irregularity than the Mono P high-pressure column packing used

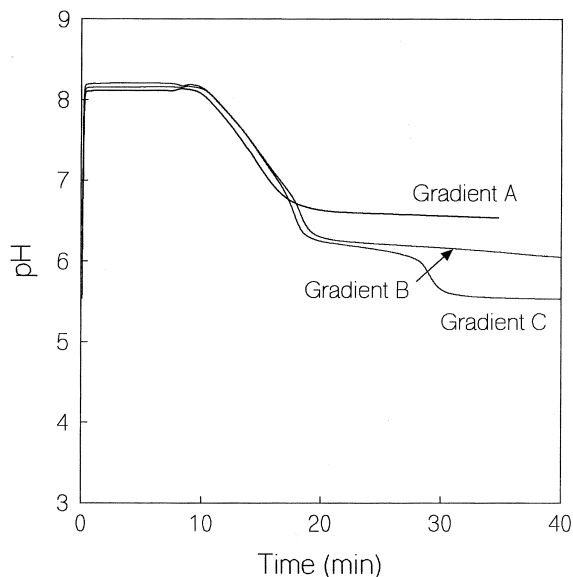


Fig. 6. Effluent pH profiles obtained using a  $5 \times 0.5$  cm I.D. Mono P column. The adsorbent was initially presaturated with a buffer containing piperazine, DEA, Tris, and imidazole each at 2 mM at a pH of 8.2 and eluted with the same mixture of species at a pH of 6.5 (gradient A), 6.0 (gradient B), and 5.5 (gradient C), and a flow-rate of 1.0 ml/min. Both the presaturation and elution buffers contained chloride as the only anion present.



in Fig. 6 would appear to be consistent with this interpretation since the latter packing is a more structurally rigid material. Evidently, for at least some types of column packings the use of poly-ampholyte buffers eliminates this behavior since pH irregularities as shown in Figs. 5 and 6 are generally not observed for either PBE 94 or Mono P when such buffers are used [5].

A hump at pH 6.2 when PBE 94 is used to produce a pH gradient with simple buffer mixtures was also observed by Logan et al. [15], although the fact that only the pH of relatively large pooled fractions collected from the column effluent were measured by these workers may have obscured the true shape of the hump in the data reported (see Fig. 4A and B of Ref. [15]). Similar pH humps were observed in the present study for several other column packings, including DEAE Sepharose FF, manufactured by Amersham Pharmacia Biotech, and ProteinPak DEAE 8HR, manufactured by Waters. In contrast, this behavior was not observed by Sluyterman and Wijdenes [4] for a polyethyleneimine derivatized Sepharose column packing nor by Logan et al. [15] for three experimental column packings used in their investigation.

Fortunately, in most cases the formation of pH humps as shown in Figs. 5 and 6 is confined to a relatively small region of the pH profile so that column packings which exhibit this behavior can nevertheless be used to produce linear or concave pH gradients with monotonically changing pH profiles over a significant pH range. For example, it was observed in this study that monotonically decreasing pH gradients without irregularities could be produced with the Mono P column packing in the ranges between pH 9.5 and 6.0 and between pH 5.5 and 4.0. Consequently, only pH gradients in these ranges were used with this column packing in the studies described below.

## 6. Experimental studies of pH gradient formation

Fig. 7 illustrates the formation of a relatively wide pH gradient which spans 3 pH units (gradient D) and three relatively narrow pH gradient which span 1.5 pH units (gradients A, E, and F). All of these

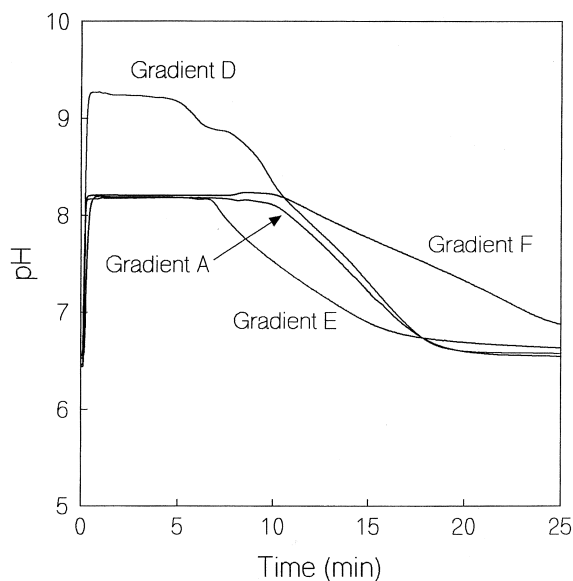


Fig. 7. Effluent pH profile obtained using a  $5 \times 0.5$  cm I.D. Mono P column at a flow-rate of 1 ml/min. For gradients A and D, the adsorbent was initially presaturated with a buffer containing piperazine, DEA, Tris, and imidazole each at 2 mM at a pH of 9.4 (gradient D) and 8.2 (gradient A) and eluted with the same mixture of species at a pH of 6.5. For gradient E, the adsorbent was initially presaturated with a buffer containing 2 mM piperazine, 2 mM DEA, 5 mM Tris, and 2 mM imidazole at a pH of 8.2 and eluted with the same mixture of species at a pH of 6.5. For gradient F, the adsorbent was initially presaturated with a buffer containing 2 mM piperazine, 2 mM DEA, 2 mM Tris, and 1 mM imidazole at a pH of 8.2 and eluted with the same mixture of species at a pH of 6.5. Both the presaturation and elution buffers contained chloride as the only anion present.

gradients were formed using a  $5 \times 0.5$  cm I.D. column containing Mono P, which is a 10- $\mu$ m commercial polyether column packing made specifically for chromatofocusing and derivatized, according to the manufacturer, with tertiary and quaternary amine functional groups. Gradients A and D in Fig. 7 employ in the elution buffer the same buffering species at the same concentrations as were used to produce all the gradients in Fig. 6. Gradients E and F, however, involve changes in the proportions of the buffering species present as compared to the other gradients shown. The specific compositions used in the elution buffers are described in the captions to Figs. 6 and 7, while the calculated buffering capacity for the elution buffers as a function of the liquid phase pH is shown in Fig. 8.

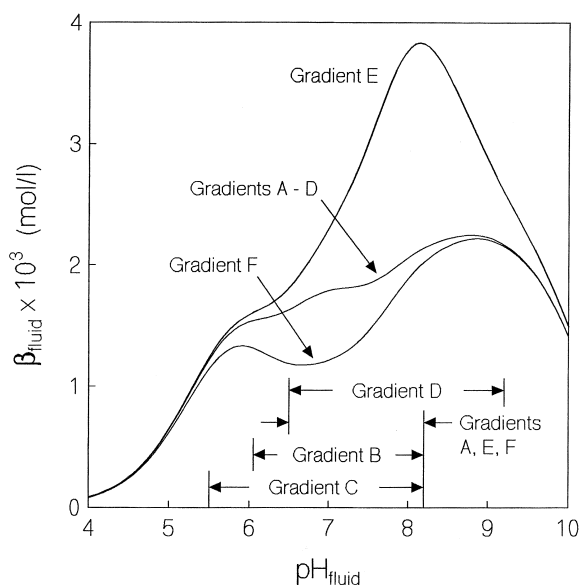


Fig. 8. Calculated buffering capacity of the mobile phases used for the experiments shown in Fig. 6 (gradients A–C) and Fig. 7 (gradients A and D–F). The pH ranges spanned by the gradients are also denoted in the figure.

Gradients A–D in Figs. 6 and 7 can be seen to be related in a manner analogous to cases 1 and 7 in Fig. 2 in that all these gradients use the same elution and presaturation buffers and are truncated versions of each other formed by titrating these buffers to different pH values. Similarly, gradients A and E in Fig. 7 can be seen to be related in a manner analogous to cases 1 and 2 in Fig. 1 in that these gradients involve changing the proportions of the buffering species present so that the gradient shape is correspondingly changed. In particular, in relation to gradient A, which is essentially a linear in shape, gradient E involves an increase in liquid-phase buffering capacity in the high-pH region that is proportionately more than the increase in the low-pH region so that a concave pH gradient is formed. In contrast, in relation to gradient A, gradient F involves a decrease in the relative liquid-phase buffering capacity, but where the relative decrease varies in a linear manner with pH, so that a less steep, but still nearly linear pH gradient is formed.

As shown in Fig. 8, the liquid-phase buffering capacity for the elution buffer corresponding to gradient A in Figs. 6 and 7 decreases by a factor of

approximately 1.4 over the range from pH 8.2 to 6.5, which is also nearly the ratio of elution times for these two pH values. According to Eqs. 1 and 2, this indicates that the buffering capacity in the adsorbed phase is relatively constant in this region. In contrast, the slightly irregular shape for gradient D in Fig. 7 in the range from between pH 9.0 and 9.5 is likely due to the maximum in the liquid phase buffering capacity that occurs at pH 8.8 and the subsequent decrease in this buffering capacity at higher pH values, and because the buffering capacity in the adsorbed phase also likely decreases at pH values greater than 9.0 since this pH is sometimes given as the upper limit to the starting pH for gradients produced using polyampholyte buffers with the Mono P column packing [21]. Gradients E and F in Fig. 7 are also seen to be in approximate agreement with Eqs. 1 and 2 since the change in the liquid phase buffering capacity across the gradient is approximately in the same ratio as the elution times corresponding to the high and low pH values for the gradient.

Fig. 7 indicates that nearly linear pH profiles can be produced using simple buffer mixtures in the range between pH 9.5 and pH 6.0, which is the majority of the working pH range of the Mono P column packing used [19,21]. In fact, gradients A, D, and F in Fig. 7 are essentially as linear as when the commercial polyampholyte chromatofocusing buffer Polybuffer 96 is used with this column packing to produce a gradient in the pH range between 9 and 6 [19]. As such, these gradient should be highly useful for the separation of proteins – a premise that will be investigated in detail in Part II of this study.

## 7. Conclusions

This study demonstrates that simple mixtures of buffering species can be employed instead of a polyampholyte elution buffer in order to produce a retained, gradual pH gradient for use in high-performance chromatofocusing. A particularly useful mixture of four buffering species is described that yields a linear pH gradient in the range between pH 9.5 and 6.0 for the case where a column packing made specifically for chromatofocusing is employed. In these systems numerical calculations as well as

simplified analytical relations based on local equilibrium theory are shown to be useful for determining the effect of the elution buffer composition on the shape of the pH gradient in terms of the buffering capacities of the adsorbed and liquid phases and for selecting the buffering species in the elution buffer in order to achieve a desired shape for the pH gradient.

## 8. Nomenclature

$B^{2+}, B^+, B^0$	Charged forms of a basic buffering species
$C_{H^+}$	Liquid phase concentration of hydrogen ion, mol/l
$C_S$	Liquid phase concentration of inert ion $S$ , mol/l
$d_p$	Particle diameter, cm
$K_a$	Acid–base dissociation constant for a monobasic species, mol/l
$K_{a1}, K_{a2}$	Acid–base dissociation constants for a dibasic species, mol/l
$K_{R_j}$	Acid–base dissociation constant for the functional group $j$ on the column packing, mol/l
$K_{S,t}$	Interphase equilibrium constant for ion $S$ based on total volume of particle
$L$	Column length, cm
$pH_{fluid}$	pH in the fluid phase
$pH_{ads}$	pH in the adsorbed phase
$q_{H^+,t}$	Hydrogen ion concentration in adsorbed phase, mol/l
$q_{R_j,t}$	Concentration of functional group in the adsorbed phase, mol/l
$q_{R^+,t}$	Total ionized functional group concentration in the adsorbed phase, mol/l particle
$q_{S,t}$	Adsorbed phase concentration of the inert ion $S$ , mol/l particle
$q_{S,t}^*$	Equilibrium adsorbed phase concentration of inert ion $S$ , mol/l particle
$t(pH)$	Transit time for a pH value, s
$v_{fluid}$	Interstitial or linear velocity, cm/s

### Greek symbols

$\alpha$	Column void volume
----------	--------------------

$\beta_{fluid}$	Buffering capacity of the liquid phase, mol/l per pH unit
$\beta_{fluid,monobasic}$	Buffering capacity of a monobasic buffering species in the liquid phase, mol/l per pH unit
$\beta_{fluid,dibasic}$	Buffering capacity of a dibasic buffering species in the liquid phase, mol/l per pH unit
$\beta_{ads}$	Buffering capacity of the adsorbed phase, defined as the change in the concentration of the inert adsorbed ion per unit change in the pH of the adsorbed phase, mol/l per pH unit
$\beta'_{ads}$	Buffering capacity of the adsorbed phase, defined as the change in the concentration of the inert ion in the adsorbed phase per unit change in the pH of the fluid phase where the fluid phase is the elution buffer under consideration, mol/l per pH unit
$\beta''_{ads}$	Buffering capacity of the adsorbed phase, defined as the change in the concentration of the inert ion in the adsorbed phase per unit change in the pH of the fluid phase where the fluid phase has an excess and constant concentration of the inert ion, mol/l per pH unit

## Acknowledgements

Support from grant CTS 9813658 from the National Science Foundation is greatly appreciated.

## References

- [1] L.A.Æ. Sluyterman, O. Elgersma, J. Chromatogr. 150 (1978) 17.
- [2] L.A.Æ. Sluyterman, J. Wijdenes, J. Chromatogr. 150 (1978) 31.
- [3] L.A.Æ. Sluyterman, J. Wijdenes, J. Chromatogr. 206 (1981) 206.
- [4] L.A.Æ. Sluyterman, J. Wijdenes, J. Chromatogr. 206 (1981) 441.
- [5] C.M. Li, T. Hutchens, in: A. Kenny, S. Fowell (Eds.), Methods in Molecular Biology, Practical Protein Chromatography, Vol. 11, Humana Press, Totowa, NJ, 1992, p. 246, Chapter 15.

- [6] J.H. Scott, K.L. Keller, H.P. Pollard, *Anal. Biochem.* 149 (1985) 163.
- [7] M.T.W. Hearn, D.J. Lyttle, *J. Chromatogr.* 218 (1981) 483.
- [8] T.W. Hutchens, C.M. Li, P.K. Besch, *J. Chromatogr.* 359 (1986) 157.
- [9] T.W. Hutchens, C.M. Li, P.K. Besch, *J. Chromatogr.* 359 (1986) 169.
- [10] Y. Liu, D.J. Anderson, *J. Chromatogr. A* 762 (1997) 47.
- [11] Y. Liu, D.J. Anderson, *J. Chromatogr. A* 762 (1997) 207.
- [12] D.D. Frey, *Biotechnol. Prog.* 12 (1996) 65.
- [13] J. Strong, D.D. Frey, *J. Chromatogr. A* 769 (1997) 129.
- [14] R. Bates, D.D. Frey, *J. Chromatogr. A* 814 (1998) 43.
- [15] K.A. Logan, I. Langerlund, S.M. Chamow, *Biotechnol. Bioeng.* 62 (1999) 208.
- [16] D.J. Krish, Mallinckrodt Baker Inc., personal communication, 1997.
- [17] J.N. Butler, *Ionic Equilibrium – A Mathematical Approach*, Addison-Wesley, Reading, MA, 1964.
- [18] D.D. Frey, A. Barnes, J. Strong, *AIChE J.* 41 (1995) 1171.
- [19] Biodirectory '99 Product Catalog, Amersham Pharmacia Biotech, Uppsala, 1999, pp. 532–533.
- [20] W.R. Melander, J. Stoveken, Cs. Horváth, *J. Chromatogr.* 185 (1979) 111.
- [21] L.G. Fägerstam, J. Lizana, U.-B. Axiö-Fredriksson, L. Wahlström, *J. Chromatogr.* 266 (1983) 523.